The Astrophysical Journal Supplement Series, 173:357–376, 2007 December

ONGOING FORMATION OF BULGES AND BLACK HOLES IN THE LOCAL UNIVERSE: NEW INSIGHTS FROM *GALEX*

Guinevere Kauffmann,[1] Timothy M. Heckman,[2] Tamás Budavári,[2] Stephane Charlot,[3] Charles G. Hoopes,[2] D. Christopher Martin,[4] Mark Seibert,[4] Tom A. Barlow,[4] Luciana Bianchi,[2] Tim Conrow,[4] José Donas,[5] Karl Forster,[4] Peter G. Friedman,[4] Young-Wook Lee,[6] Barry F. Madore,[7,8] Bruno Milliard,[5] Patrick F. Morrissey,[4] Susan G. Neff,[9] R. Michael Rich,[10] David Schiminovich,[11] Todd Small,[4] Alex S. Szalay,[2] Ted K. Wyder,[4] and Sukyoung K. Yi[6]

Received 2006 July 18; accepted 2006 September 13

ABSTRACT

We analyze a volume-limited sample of massive bulge-dominated galaxies with data from both the Sloan Digital Sky Survey and the *Galaxy Evolution Explorer* (*GALEX*) satellite. The galaxies have central velocity dispersions greater than 100 km s^{-1} and stellar surface mass densities that lie above the value where galaxies transition from actively star-forming to passive systems. The sample is limited to redshifts $0.03 < z < 0.07$. At these distances, the SDSS spectra sample the light from the bulge-dominated central regions of the galaxies. The *GALEX* NUV data provide high sensitivity to low rates of *global* star formation in these systems. Our sample of bulge-dominated galaxies exhibits a much larger dispersion in NUV $-$ r color than in optical $g - r$ color. The dispersion increases for galaxies with smaller central velocity dispersions, and nearly all of the galaxies with bluer NUV $-$ r colors are active galactic nuclei (AGNs). Both *GALEX* images and SDSS color profiles demonstrate that the excess UV light is nearly always associated with an extended disk. When comparing fiber-based estimates of stellar age to global ones, we find that galaxies with red outer regions almost never have a young bulge or a strong AGN. Galaxies with blue outer regions have bulges and black holes that span a wide range in age and accretion rate. Galaxies with young bulges and strongly accreting black holes almost *always* have blue outer disks. The black hole growth rate correlates much more strongly with the age of the stars in the bulge than in the disk. Our suggested scenario is one in which the source of gas that builds the bulge and black hole is a low-mass reservoir of cold gas in the disk. The presence of this gas is a necessary but not sufficient condition for bulge and black hole growth. Some mechanism must transport this gas inward in a time variable way. The disk gas itself is likely to be the result of the accretion of gas from an external source. As the gas in the disk is converted into stars, galaxies will turn red, but further inflow can bring them back into the blue NUV $-$ r sequence.

Subject headings: galaxies: active — galaxies: bulges — galaxies: elliptical and lenticular, cD — galaxies: formation

1. INTRODUCTION

The formation and evolutionary history of massive bulge-dominated galaxies has been a subject of considerable controversy over the past decade. On the one hand, the colors and detailed spectral energy distributions of these galaxies indicate that their stellar populations are predominantly old and metal-rich (see Renzini 2006 for a recent review). The dispersion in spectral properties between different systems is small, indicating that the stars in different galaxies were formed at roughly similar epochs and less than a few gigayears after the big bang (e.g., Bower et al. 1992) On the other hand, a theoretical paradigm for the assembly of structure in the universe has emerged in recent years, which at first sight has appeared to contradict this observational data. According to this paradigm, the largest structures in the universe form *hierarchically* through the merging of small virialized condensations (halos) to form larger and larger systems. This means that the dark matter halos that host massive bulge-dominated galaxies are predicted to have assembled relatively recently. In addition, a significant fraction of these galaxies are expected to reside at the centers of massive halos, where gas is expected to reach high enough densities to be able to cool through radiative processes. The predicted cooling rates in these halos are high enough to produce a population of young stars that should be easily detectable in the spectra of their central galaxies (see,e.g., Kauffmann et al. 1993).

In order to resolve this so-called "cooling crisis," a number of recent models invoke feedback from the active galactic nuclei (AGNs) in massive galaxies. Energy from the material accreting onto the central supermassive black hole is transported to the gas surrounding the galaxy either by jets, which are known to exist in radio galaxies (e.g., Churazov et al. 2001; Ruszkowski et al. 2004; Best et al. 2005; Croton et al. 2006), or by powerful outflows that are hypothesized to be triggered during galaxy-galaxy mergers (Granato et al. 2004; Di Matteo et al. 2005).

[1] Max-Planck-Institut fur Astrophysik, Karl-Schwarzschild-Strasse 1, D-85748 Garching bei Munchen, Germany.
[2] Department of Physics and Astronomy, Johns Hopkins University, 3400 North Charles Street, Baltimore, MD 21218.
[3] Institut d'Astrophysique de Paris, UMR 7095, 98 bis Boulevard Arago, F-75014 Paris, France.
[4] Division of Physics, Mathematics, and Astronomy, California Institute of Technology, Pasadena, CA 91125.
[5] Laboratoire d'Astrophysique de Marseille, BP 8, Traverse du Siphon, 13376 Marseille Cedex 12, France.
[6] Center for Space Astrophysics, Yonsei University, Seoul 120-749, Korea.
[7] Observatories of the Carnegie Institution of Washington, 813 Santa Barbara Street, Pasadena, CA 91101.
[8] NASA/IPAC Extragalactic Database, California Institute of Technology, MC 100-22, 770 South Wilson Avenue, Pasadena, CA 91125.
[9] Laboratory for Astronomy and Solar Physics, NASA Goddard Space Flight Center, Greenbelt, MD 20771.
[10] Department of Physics and Astronomy, University of California at Los Angeles, 8965 Mathematical Sciences Building, Los Angeles, CA 90095.
[11] Department of Astronomy, Columbia University, MC 2456, 550 West 120th Street, New York, NY 10027.

All these models are highly schematic, so it is valuable to use observational data to provide a more detailed understanding of the cooling, star formation, and heating processes that regulate the evolution of massive galaxies. Although the present-day star formation rates in massive galaxies galaxies are constrained to be low on average, there is observational evidence that stars do continue to form in a subset of these systems. The optical spectra of central cluster galaxies frequently exhibit line emission and blue continua (McNamara & O'Connell 1989; Cardiel et al. 1998; Crawford et al. 1999). Excess ultraviolet light has also been detected in number of central cluster galaxies (Hicks & Mushotzky 2005). The inferred star formation rates in these objects are similar to rate at which gas is measured to be cooling at the very centers of the clusters using X-ray data from the *Chandra X-Ray Observatory* and *XMM-Newton* satellites (McNamara 2004).

Recently, near- and far-ultraviolet photometry from the *Galaxy Evolution Explorer* (*GALEX*) has been assembled for a large sample of galaxies from the Sloan Digital Sky Survey (SDSS). The advantage of studying galaxies at ultraviolet wavelengths is that their UV luminosities are very sensitive to low levels of residual star formation. The disadvantage is that rest-frame ultraviolet data can only be obtained from space for galaxies at low redshifts, so until recently the available galaxy samples have been small. Yi et al. (2005) and Rich et al. (2005) presented analyses of the UV/optical color-magnitude relation of two samples of early-type galaxies selected from the first matched *GALEX*/SDSS sample. These studies found that the UV/optical colors of these galaxies exhibit significantly larger scatter than their optical colors. The main conclusion was that low-level residual star formation was common during the last billion years, even in bright early-type galaxies. Rich et al. (2005) also noted that early-type galaxies with AGNs were much more likely than quiescent galaxies to show blue UV/optical colors. Possible implications of the above results for models of elliptical galaxy formation have been considered in recent papers by Kaviraj et al. (2005, 2006), Martin et al. (2006), and Schawinski et al. (2007, 2006).

We note, however, that Boselli et al. (2005) carried out an analysis of UV properties of a sample of nearby elliptical galaxies in the Virgo cluster and found rather tight color-magnitude relations for the objects in their sample. The ellipticals in this sample were selected using high-quality photographic plates taken with the DuPont telescope at Las Campanas Observatory. The differences between the Boselli et al. analysis and the studies that use the SDSS imaging data to select early-type galaxies suggest that UV properties of early-type galaxies may be quite sensitive to the exact selection criteria used to define the different samples.

In this paper, we adopt a different approach. Using a parent sample of galaxies with *GALEX* detections that are matched to the SDSS Data Release 4 (DR4) sample, we have constructed a volume-limited sample of bulge-dominated galaxies in the local universe with near-UV and optical photometry, as well as optical spectroscopy from the SDSS. Unlike the previous studies, our sample is selected on the basis of bulge velocity dispersion and *not* on the basis of conventional Hubble type. Our sample is also limited to lie at redshifts less than 0.07. At these distances the galaxies subtend a large enough solid angle on the sky to enable us to study the radial distributions of the young stars in the galaxies using both the *GALEX* and the SDSS images. In addition, the spectra of these galaxies have very high signal-to-noise ratios, enabling us to accurately deconvolve even intrinsically weak emission lines from the underlying stellar absorption continuum and to study the properties of AGNs in these objects. In § 2 we describe the details of our sample selection. In § 3 we compare the UV/optical color relations of bulge-dominated galaxies with the "traditional" relations defined only in the optical. In § 4 we analyze the spatial distribution of the young stars in galaxies with blue NUV $-$ r colors. In § 5 we examine the link between low levels of ongoing star formation and AGN activity in our sample. In § 6, we study the stellar mass profiles of the galaxies in our sample. Finally, in § 7 we summarize and interpret our results.

2. THE SAMPLE

2.1. *Ultraviolet Data*

Since its launch in 2003 April, *GALEX* has been conducting several surveys of the UV sky. Details on the *GALEX* mission and surveys are given in Martin et al. (2005). In this paper we make use of the *GALEX* Medium Imaging Survey (MIS). MIS exposures are typically 1500 s long and reach a limiting magnitude $m_{\rm AB} \sim 23$. Our data are taken from the *GALEX* MIS IR1.1(+GR1) data release. The *GALEX* data include far-ultraviolet (FUV; $\lambda_{\rm eff} = 1528$ Å, $\Delta\lambda = 268$ Å) and near-ultraviolet (NUV; $\lambda_{\rm eff} = 2271$ Å, $\Delta\lambda = 732$ Å) images with a circular field of view with radius $\sim 38'$. The spatial resolution is $\sim 5''$. Details of the *GALEX* satellite and data characteristics can be found in Morrisey et al. (2005). The data were processed through the *GALEX* reduction pipeline at the California Institute of Technology. The pipeline reduces the data and automatically detects, measures, and produces catalogs of FUV and NUV fluxes for sources in the *GALEX* images.

2.2. *Optical Data*

The *GALEX* catalogs were then matched to the SDSS Fourth Data Release (DR4; Adelman-McCarthy et al. 2006) spectroscopic sample. The matching procedure is described in Seibert et al. (2005). Matching to SDSS provides a variety of photometric parameters in the u, b, v, r, i, and z photometric passbands, as well as spectroscopic redshifts for a sample of 51,246 galaxies with UV detections. In this analysis, we exclude galaxies located more than $30'$ from the MIS field centers, because the photometry is not as reliable near the boundaries.

In addition to the SDSS photometric parameters, a large number of galaxy parameters derived from the SDSS spectra are available in the value-added catalogs at the SDSS Web site at the Max Planck Institute for Astrophysics.[12] From these catalogs we use the stellar masses, stellar velocity dispersions, the spectral indices $D_n(4000)$ and $H\delta_A$, the equivalent width of the Hα emission line [EQW(Hα)], and the AGN classifiers. For detailed information about the derivation of these quantities, see Kauffmann et al. (2003a, 2003c), Brinchmann et al. (2004), and Tremonti et al. (2004). Throughout this paper we have assumed $H_0 = 70$ km s^{-1} Mpc^{-1}, $\Omega_m = 0.3$, and $\Omega_\Lambda = 0.7$.

The aim of the present analysis is to study a volume-limited sample of bulge-dominated galaxies. It is thus important to make sure that our sample, which is initially selected in the UV, is not biased *against* galaxies with no ongoing star formation. In Figure 1, we show how the NUV $-$ r and $g - r$ colors of galaxies depend on the fraction of the stellar mass that was formed in the past gigayear. These curves were generated using the Bruzual & Charlot (2003) GALAXEV code assuming a solar metallicity stellar population and smooth, exponentially declining star formation histories with varying e-folding times. As can be seen from the plot, as the fraction of young stars in the galaxy goes to zero, the NUV $-$ r colors are predicted to saturate at a value of around 6.5. The figure also shows that the NUV $-$ r color remains sensitive

[12] See http://www.mpa-garching.mpg.de/SDSS.

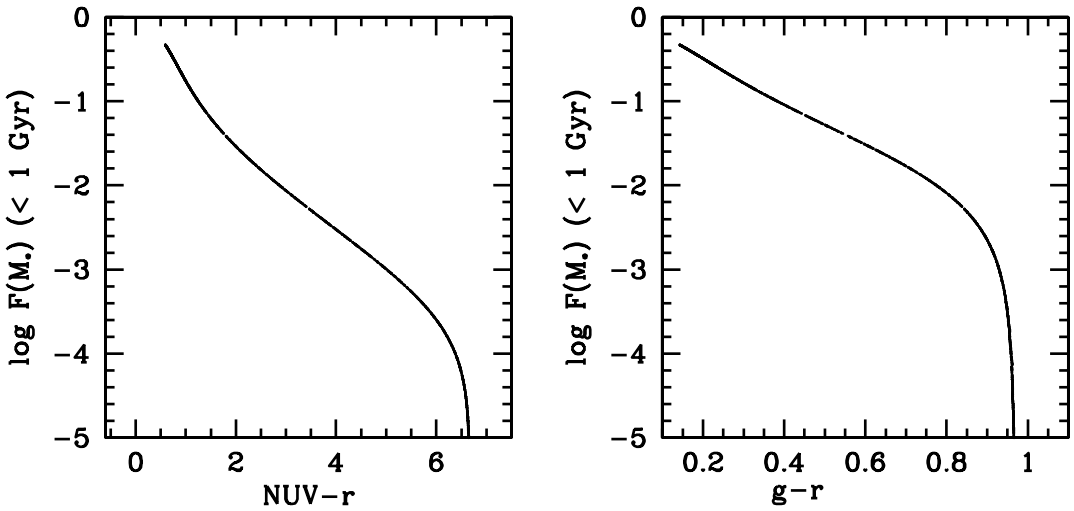

FIG. 1.—Fraction of mass in stars in the galaxy formed in the last gigayear is plotted as a function of NUV − *r* (*left*) and *g* − *r* color (*right*) for model galaxies that gave smooth, exponentially declining star formation histories.

to a much lower level of recent star formation than the optical $g - r$ color. Since our *GALEX* sample is limited at $m_{AB} = 23$, Figure 1 suggests that an *r*-band magnitude limit of 16.5 (i.e., 1.2 mag brighter than the limit of the main spectroscopic sample) is required in order to ensure that our sample is not biased against galaxies with the very oldest stellar populations.

Figure 2 (*top left*) shows the NUV − *r* color distribution of galaxies with $r < 16.5$ and NUV < 23 in our sample. We use SDSS model magnitudes, which are well matched to the AUTO/Kron magnitudes output by the *GALEX* pipeline. The magnitudes have also been corrected for foreground extinction using the values of $E(B - V)$ given by Schlegel et al. (1998) and the Cardelli et al. (1989) reddening curve. As can be seen, the color distribution is clearly bimodal. The population of red galaxies is peaked at NUV − $r \sim 6$, and there are very few galaxies with NUV − $r > 6.5$. This gives us confidence that our sample is indeed complete in NUV − *r* color space. In the next two panels, we plot the stellar masses and the stellar velocity dispersions (measured within the 3″ fiber aperture) of the red galaxies with NUV − $r > 4.5$ as a function of their redshifts. These red objects are the most difficult to detect in the UV, and they also have the highest *r*-band stellar mass-to-light ratios, so they determine the effective completeness limit of our sample. Figure 2 shows that if we limit the sample to lie in the redshift range $0.03 < z < 0.07$, we are complete down to $\log M_\star \sim 10.4$ and $\log \sigma \sim 2.05$.

We note that at $z \sim 0.05$, the SDSS fiber aperture subtends a physical scale of only 3.2 kpc. The physical quantities that are measured from the spectra are thus relevant to the central bulge-dominated regions of the galaxy. Throughout this paper, we interpret spectral quantities such as $D_n(4000)$, $H\delta_A$, and EQW(Hα) as measures of the age of the stellar population *in the bulge*. The NUV − *r* and *g* − *r* colors, on the other hand, are sensitive to the age of the stellar population of the galaxy as a whole.

In Figure 2 (*bottom right*) we plot the stellar surface mass density $\mu_\star$ as a function of stellar velocity dispersion for galaxies with $\log M_\star > 10.4$, $\log \sigma > 2.05$, $r < 16.5$, NUV < 23, and $0.03 < z < 0.07$. This sample includes 1375 galaxies. The surface mass density $\mu_\star$ is defined as $\mu_\star = (0.5M_\star)/(\pi R50z)^2$, where *R*50*z* is the half-light radius of the galaxy in the *z* band. As discussed in Kauffmann et al. (2003b, 2006), there is a sharp transition in the mean stellar age of galaxies at a stellar surface mass density $\mu_\star$ of around $10^{8.5}\ M_\odot\ \mathrm{kpc}^{-2}$. Galaxies with surface densities lower than this value have on average formed their stars at a constant rate for a Hubble time; galaxies with surface densities higher than this value have little or no ongoing star formation. Figure 2 shows that essentially all galaxies in our sample defined at $\log \sigma > 2.05$ have surface densities greater than the transition value. The range of densities spanned by the objects in our sample is also very similar to that of elliptical galaxies (Bernardi et al. 2003), and hence it is meaningful to refer to these objects as "bulge-dominated" systems.

We also find that 85% of the galaxies in our sample have *r*-band concentration indices ($C = R90/R50$) greater than 2.6. Strateva et al. (2001) and Shimasaku et al. (2001) have studied how this index relates to "by eye" classification into Hubble type. These authors find that $C = 2.6$ marks a reasonably robust division between early-type galaxies (E/S0/Sa) and the late-type spiral population. Note that we choose not to apply further cuts to exclude the minority of later type galaxies in our sample. The aim of the present paper is to examine possible evolutionary links between different galaxy populations at fixed bulge velocity dispersion or mass. It is thus critical to ensure that our sample is complete at a given value of σ.

3. COLOR RELATIONS

In Figure 3, we plot the NUV − *r* and *g* − *r* colors of the galaxies in our sample as a function of the stellar velocity dispersion measured within the SDSS fiber. The points have been color coded according the emission-line properties of the galaxies. Galaxies with emission lines that are too weak to permit a secure classification are colored in black, AGNs are colored in red, and star-forming galaxies are colored in blue. As can be seen, the scatter in the NUV − r/σ relation is substantially larger than the scatter in the $g - r/\sigma$ relation. The scatter increases at lower values of σ in both diagrams. It is striking that at velocity dispersions greater than ~125 km s^{-1}, almost all the galaxies with blue NUV − *r* colors are classified as AGNs. There are only a small number of galaxies with emission-line ratios typical of star-forming galaxies and these all have small central velocity dispersions. These results are quantified in more detail in Figure 4, where we plot color distributions in different ranges of stellar velocity dispersion. The black histograms represent the results for the full sample, while the red and blue histograms show the contributions from AGN and star-forming galaxies respectively.

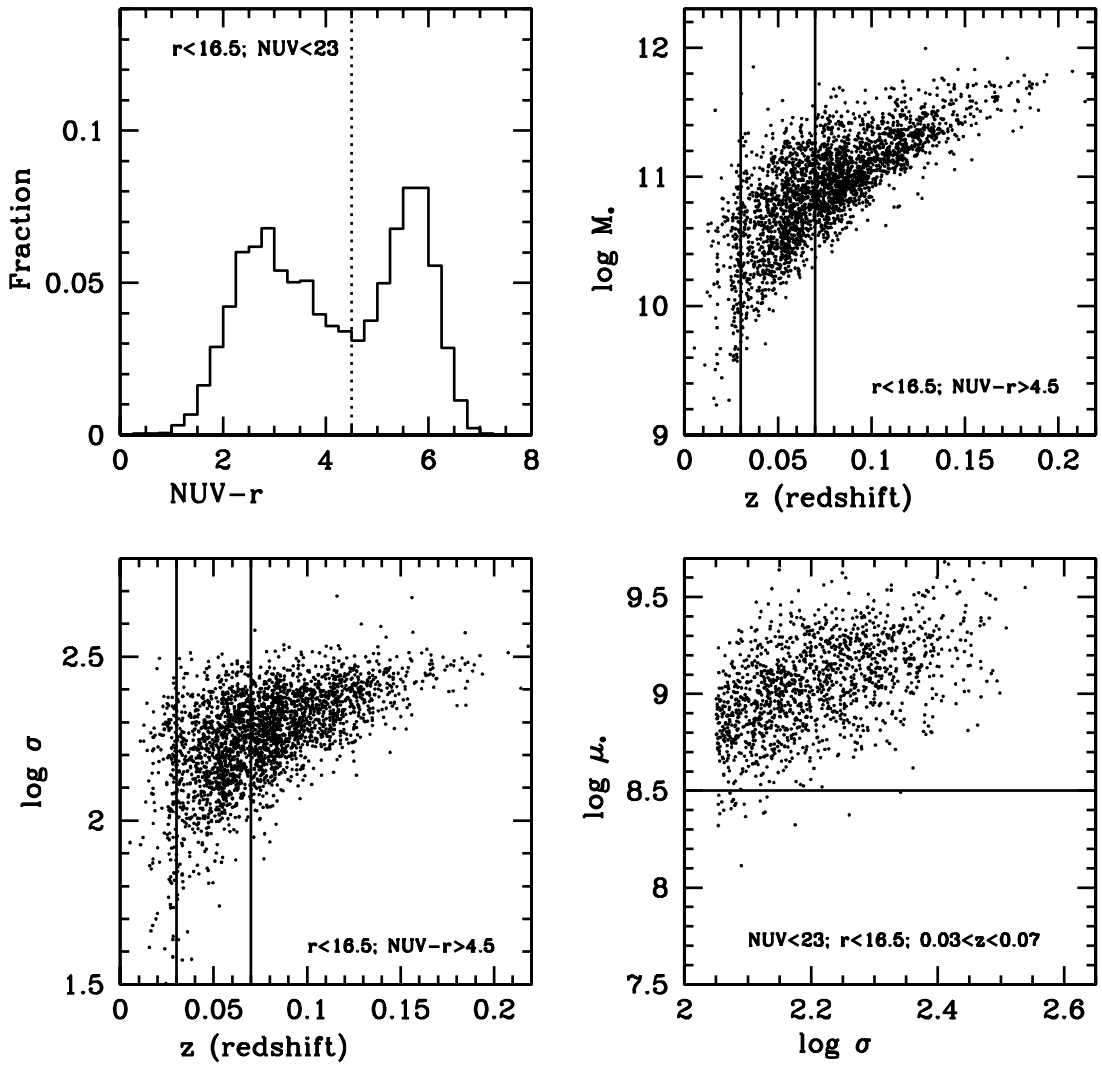

FIG. 2.—*Top left*: NUV − r color distribution of galaxies with with $r < 16.5$ and NUV < 23 in our sample. *Top right, bottom left*: Stellar mass and stellar velocity dispersion plotted as a function of redshift for galaxies with NUV $- r > 4.5$, $r < 16.5$, and NUV < 23. *Bottom right*: Stellar surface mass density is plotted as a function of stellar velocity dispersion for galaxies with $\log M_\star > 10.4$, $\log \sigma > 2.05$, $r < 16.5$, NUV < 23, and $0.03 < z < 0.07$. The horizontal line indicates the "transition" value of $\mu_\star$ between galaxies with ongoing star formation and galaxies where star formation has largely shut down.

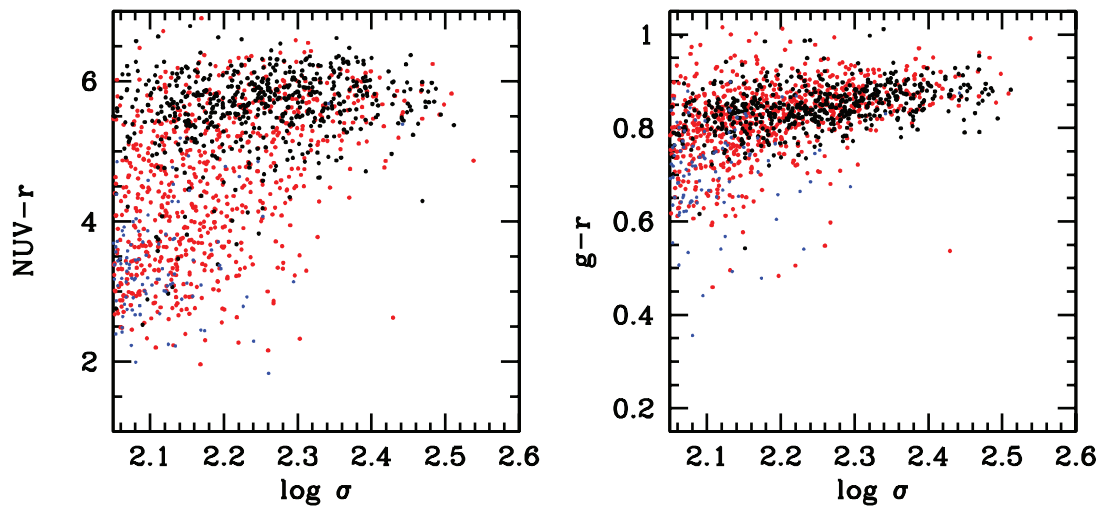

FIG. 3.—Relations between NUV − r and $g - r$ colors and central stellar velocity dispersion for the galaxies in our sample. Black dots indicate galaxies with emission lines that are too weak to classify, red dots show AGNs, and blue dots show star-forming galaxies.

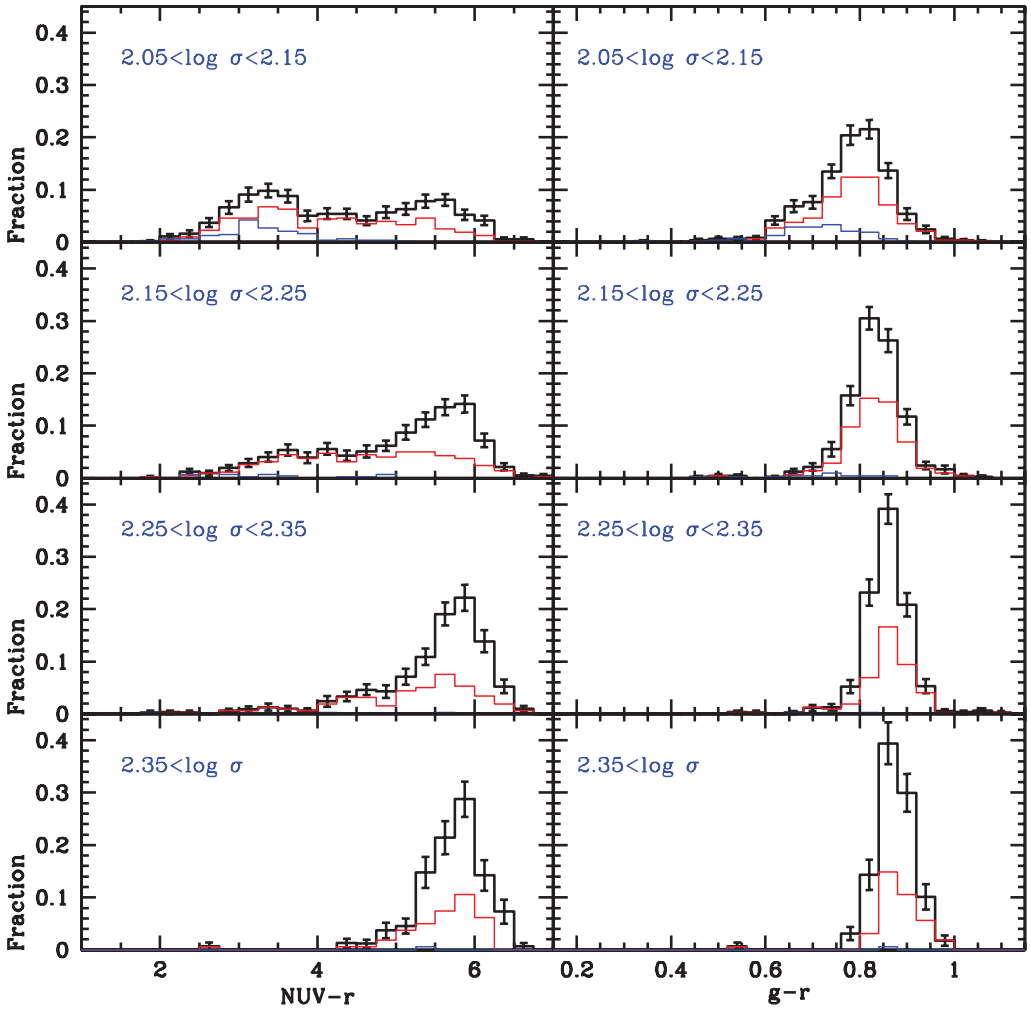

FIG. 4.—Distribution of NUV − r and $g - r$ colors in different ranges of central velocity dispersion. Black histograms are for the whole sample, red shows the contribution from AGNs, and blue shows that from star-forming galaxies.

Figure 5 examines the relations between four different stellar population indicators: the NUV − r color, the $g - r$ color, the 4000 Å break index $D_n(4000)$, and the equivalent width of the Hα emission line. As discussed in the previous section, the NUV − r and $g - r$ colors are measures of the stellar populations of the galaxy as a whole, whereas $D_n(4000)$ and EQW(Hα) probe the stellar populations within the central bulge-dominated region. (Note that for galaxies classified as AGNs the Hα will be sensitive to the ionizing flux from the central source, as well as the H II regions in the galaxy.) Figure 5 shows that there is a tight but strongly nonlinear correlation between the $g - r$ and NUV − r colors. As shown in Figure 1, galaxies with NUV − r colors in the range 4–6 have formed less than 0.3% of their stars over the last gigayear. The $g - r$ optical colors are completely insensitive to such low levels of star formation; this is why $g - r$ is flat over this range in NUV − r color. The two spectral indicators measured within the fiber [$D_n(4000)$ and EQW(Hα)] also exhibit a tight correlation. At fixed $D_n(4000)$, AGNs (*red*) scatter to slightly higher Hα equivalent widths than star-forming galaxies (*blue*), consistent with the notion that radiation from the active nucleus contributes to the ionization of the Hα line. Nevertheless, the relation between the two indicators is still quite tight for both classes of object. However, when we plot the fiber indicators as a function of the global NUV − r colors, we see a huge scatter. Galaxies with NUV − r colors in the range 2–4 have Hα equivalent widths that differ by more than an order of magnitude, and $D_n(4000)$ values that span the entire dynamic range of the index.

The most obvious explanation for this enormous scatter is that the *UV light does not trace the stellar population in the bulge*. As we have noted previously, our sample is chosen to lie at redshifts below 0.07 and the physical aperture subtended by the SDSS fiber is only a few kiloparsecs. The hypothesis that the UV light does not originate from the bulge is consistent with recent *GALEX* studies of very nearby galaxies, which indicate that a significant fraction of the UV light originates in the outer disks of galaxies (Thilker et al. 2005). Popescu et al. (2005) showed that the UV–to–far-infrared flux ratio in the galaxy M101 is a strong function of radius, with values monotonically decreasing from ∼4 in the nuclear region to nearly zero at the edge of the optical disk. In the next section, we prove that the UV light is biased toward the outer regions of the galaxies in our sample by analyzing their mean optical radial color profiles as a function of their global NUV − r colors.

4. COLOR PROFILES

The SDSS photometric pipeline extracts azimuthally averaged radial surface brightness profiles for all the objects in the survey. In the catalogs, this is given as the average surface brightness

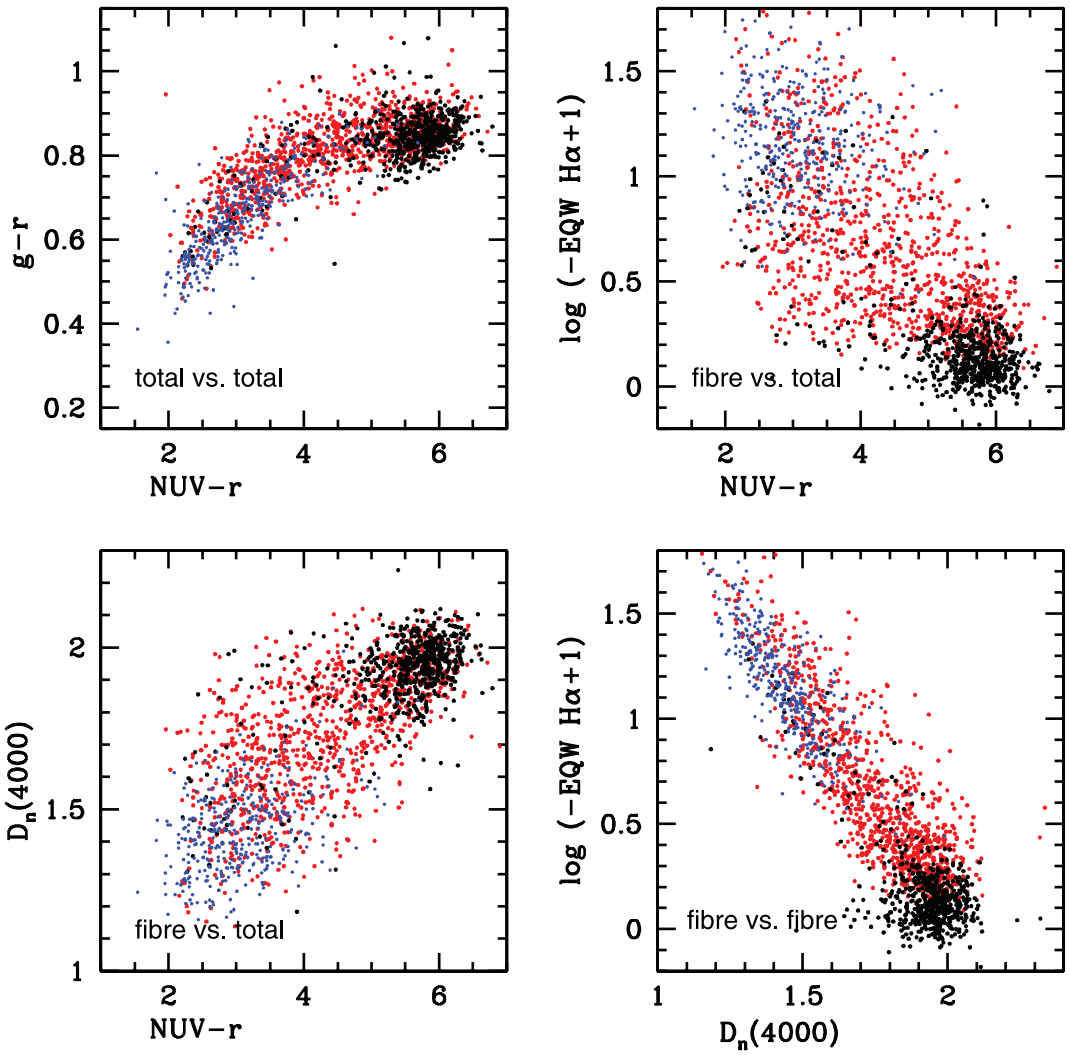

FIG. 5.—Relations between four different stellar population indicators: the NUV − r color, the $g - r$ color, the 4000 Å break index $D_n(4000)$, and the equivalent width of the Hα emission line. Galaxies with emission lines that are too weak to classify are shown as black dots, AGNs are shown in red, and star-forming galaxies are plotted in blue.

in a series of annuli with fixed angular dimension. Results are stored in the u, g, r, i, and z bands, so it is simple to compute radial color gradients for the galaxies in our sample. In Figure 6, we plot $g - i$ as a function of physical radius for UV-bright (*top panels*) and UV-faint (*bottom panels*) galaxies with stellar velocity dispersions in the range $2.05 < \log \sigma < 2.25$. The average profile is shown as a solid line; the dashed lines indicate the 10th to 90th percentiles in the range of color spanned by the galaxies at a given radius. The color profiles are smooth because we average over samples of between 100 and 300 objects. We only plot results out to radii where the photometric errors in the flux contained within the radial bin are less than ~10%.

It is clear from Figure 6 that UV-bright galaxies have very similar central colors to UV-faint galaxies but are significantly bluer in their outer regions. UV-bright galaxies with strong emission lines in their central regions exhibit a larger scatter in their central $g - i$ colors, but their *average* nuclear colors are very similar to their UV-bright counterparts with weak emission lines. As was noted in the previous section, essentially all UV-bright galaxies with central stellar velocity dispersions in this range are classified as AGNs. In the bottom two panels, we compare the color profiles of UV-faint galaxies that are classified as AGN with those with emission lines that are too weak to classify. The color profiles of the two kinds of galaxy are very similar. UV-faint AGNs are slightly bluer in their outer regions on average.

In Figures 7 and 8, we show a montage of SDSS g, r, and i and *GALEX* FUV and NUV color images of bulge-dominated galaxies with blue NUV − r colors (NUV − $r < 4.5$). In Figure 9 we show a sample of bulge-dominated galaxies with red NUV − r colors (NUV − $r > 5$) for comparison. All the galaxies are selected to lie between redshifts 0.04 and 0.06, and they all have central stellar velocity dispersions in the range $2.1 < \log \sigma < 2.4$. Each postage-stamp image is 100″ on a side, which corresponds to a physical scale of ~100 kpc. In Figure 7 we show galaxies with NUV − $r < 4.5$ and low Hα equivalent widths measured within the fiber [EQW(Hα) > −2 Å]. Figure 8 shows galaxies with NUV − $r < 4.5$ and EQW(Hα) < −7 Å (note that essentially all of these are AGNs). There is no explicit emission-line cut in Figure 9, but as shown in Figure 5, almost all galaxies with red NUV − r colors have low emission-line equivalent widths.

The SDSS color images have been produced using an algorithm described in Lupton et al. (2004). The algorithm uses an "arcsinh

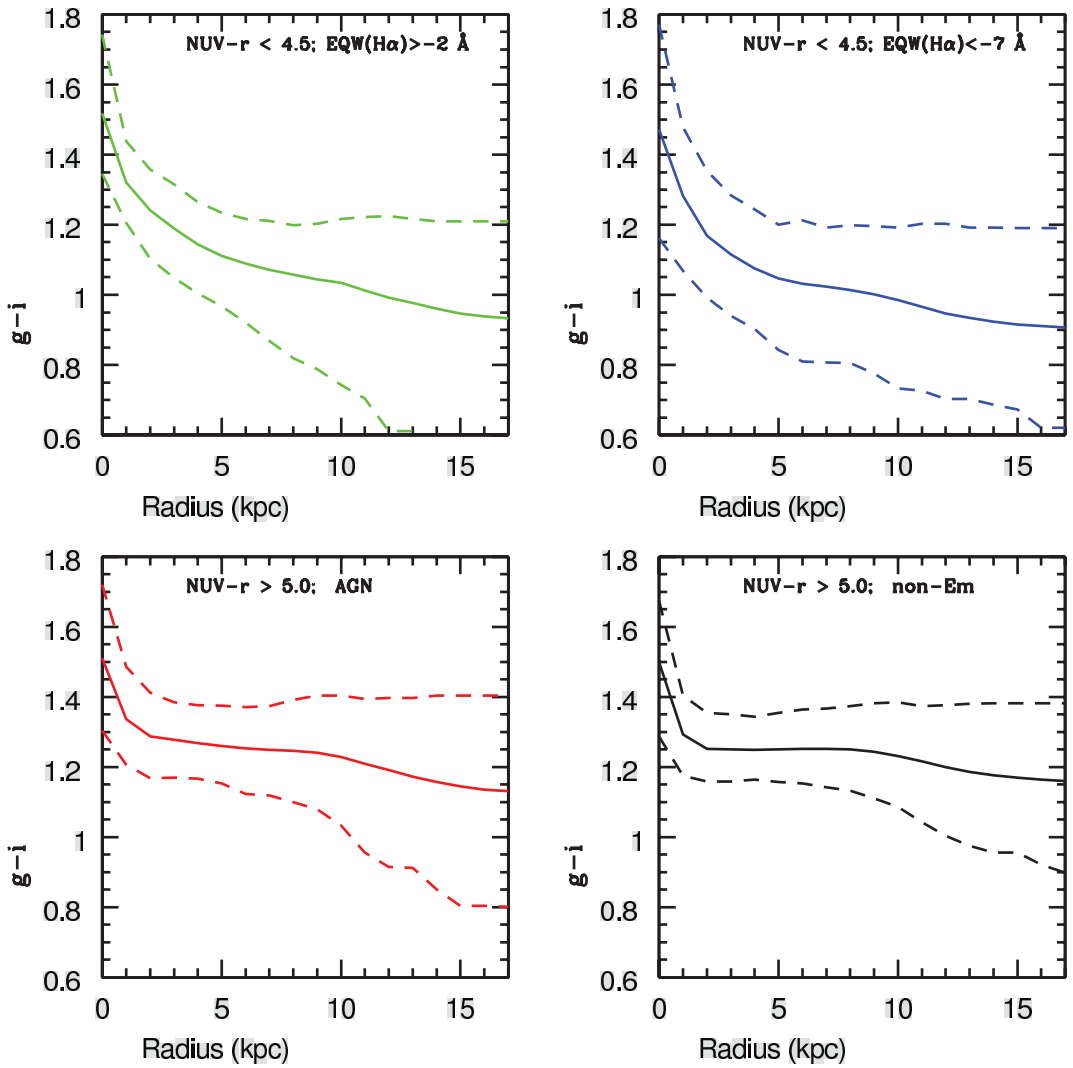

FIG. 6.—Color $g - i$ plotted as a function of physical radius for UV-bright (*top panels*) and UV-faint (*bottom panels*) galaxies with stellar velocity dispersions in the range $2.05 < \log \sigma < 2.25$. The average profile is shown as a solid line; the dashed lines indicate the 10–90 percentiles in the range of color spanned by the galaxies at a given radius.

stretch" that allows faint, low surface brightness features in a galaxy to be displayed, while simultaneously preserving the structure of the bright, high surface brightness components. Even at recessional velocity of 15,000 km s^{-1}, these galaxies display a rich complexity of structure in the SDSS images, with outer rings, bars, and spiral structure clearly visible in many objects.[13] The *GALEX* UV images have considerably lower spatial resolution than the SDSS images, but they make it clear that the UV light is extended over large spatial scales. In Figure 7, there are galaxies where the UV appears to extend beyond the optical radius of the galaxy, out to galactic radii as large as 40–50 kpc. The UV-bright galaxies displayed in Figure 8 have higher UV surface brightnesses than those in Figure 7, but the UV emission still clearly extends over the entire region traced by the optical light, and sometimes beyond. On the other hand, the UV-faint galaxies displayed in Figure 9 occasionally display some extended emission, but in most cases the UV light appears to be concentrated in the same bulge-dominated regions of the galaxies as the optical light.

[13] Note that if the same galaxies are viewed at larger distances, this structure becomes increasingly difficult to see in the SDSS postage-stamp images. We inspected SDSS images of galaxies with the same range of central velocity dispersions at $z = 0.1$, and we found that although outer disks are sometimes visible, it is no longer possible to discern star-forming regions in the images.

5. WHAT IS THE LINK BETWEEN THE UV EMISSION AND THE AGN ACTIVITY?

In § 3 we showed that bulge-dominated galaxies with blue NUV − *r* colors almost always have central emission-line spectra characteristic of ionization by an active nucleus. In § 4 we showed that the UV emission in bulge-dominated galaxies is a tracer of young stars in the *outer* region of the galaxy. This leads us to the following question: what, if any, is the physical connection between this extended UV emission and the activity in the nucleus of the galaxy?

In order to address this issue, it is necessary to move beyond simple classification of the galaxies in our sample into AGNs and and non-AGNs. Heckman et al. (2004) introduced the [O III] emission-line luminosity as an indicator of the rate at which matter is accreting onto the central supermassive black hole. There are two reasons why the [O III] emission-line luminosity is believed to be a good indicator of accretion rate. (1) [O III] emission is relatively weak in metal-rich H II regions. (2) In type I Seyfert galaxies and quasars, the [O III] line luminosity is well correlated

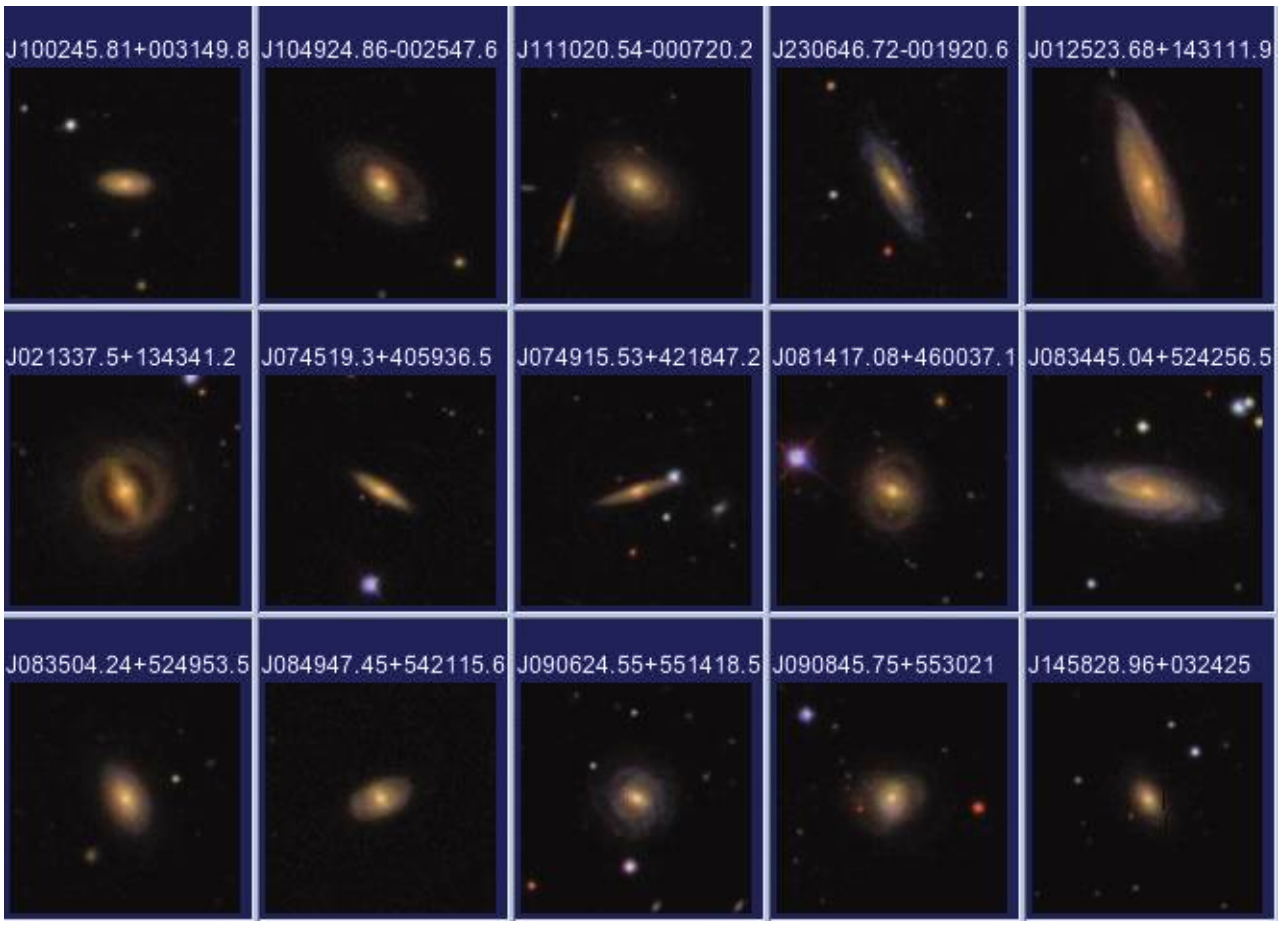

FIG. 7.—SDSS (*first group*) and *GALEX* (*second group*) images of UV-bright galaxies with low central Hα equivalent widths. Each postage-stamp image is 100″ on a side, which correpsonds to a physical scale of $\sim$100 kpc at these redshifts ($z = 0.04-0.06$). Note that the UV disks are sometimes nearly as large as the entire field. The SDSS fiber diameter is 3″.

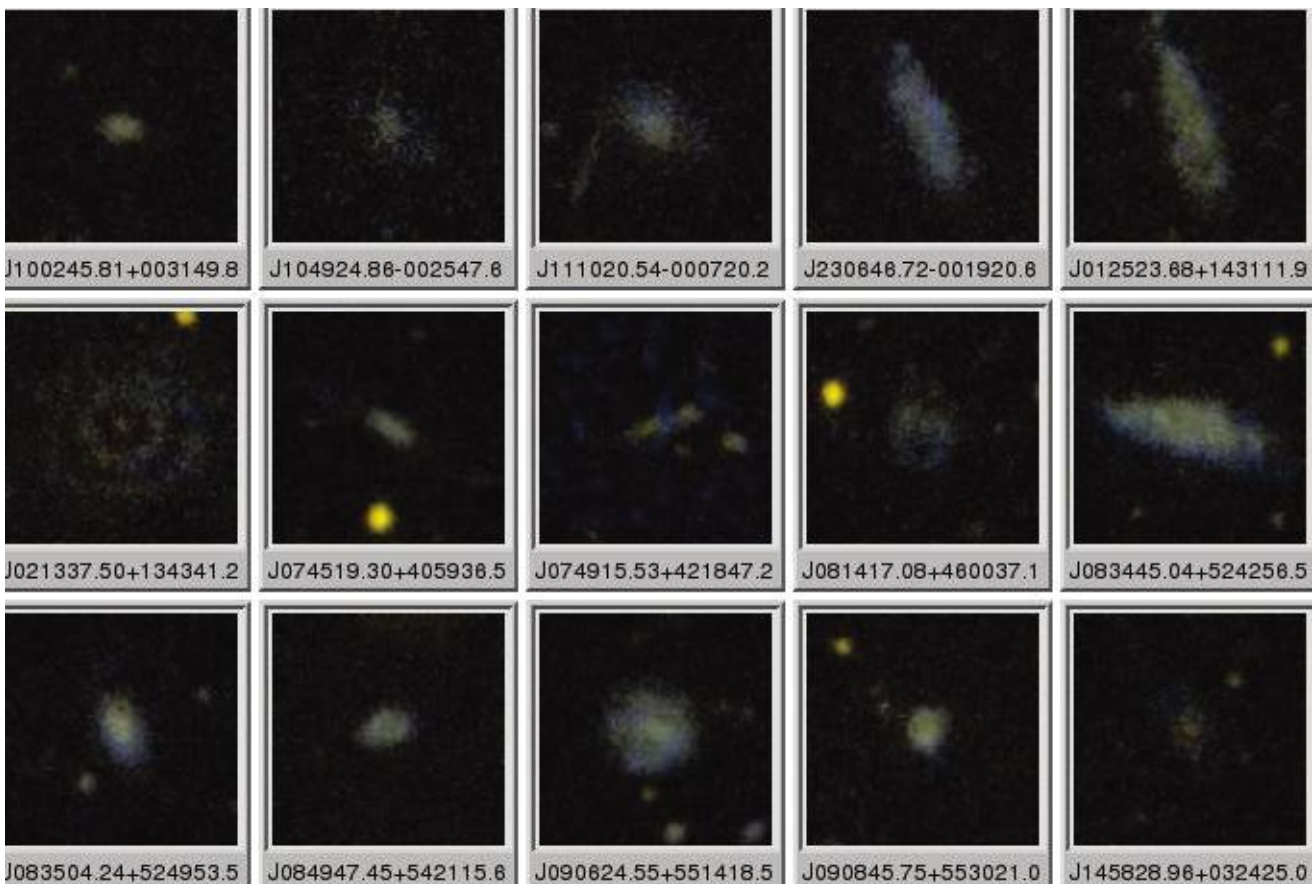

FIG. 7.—*Continued*

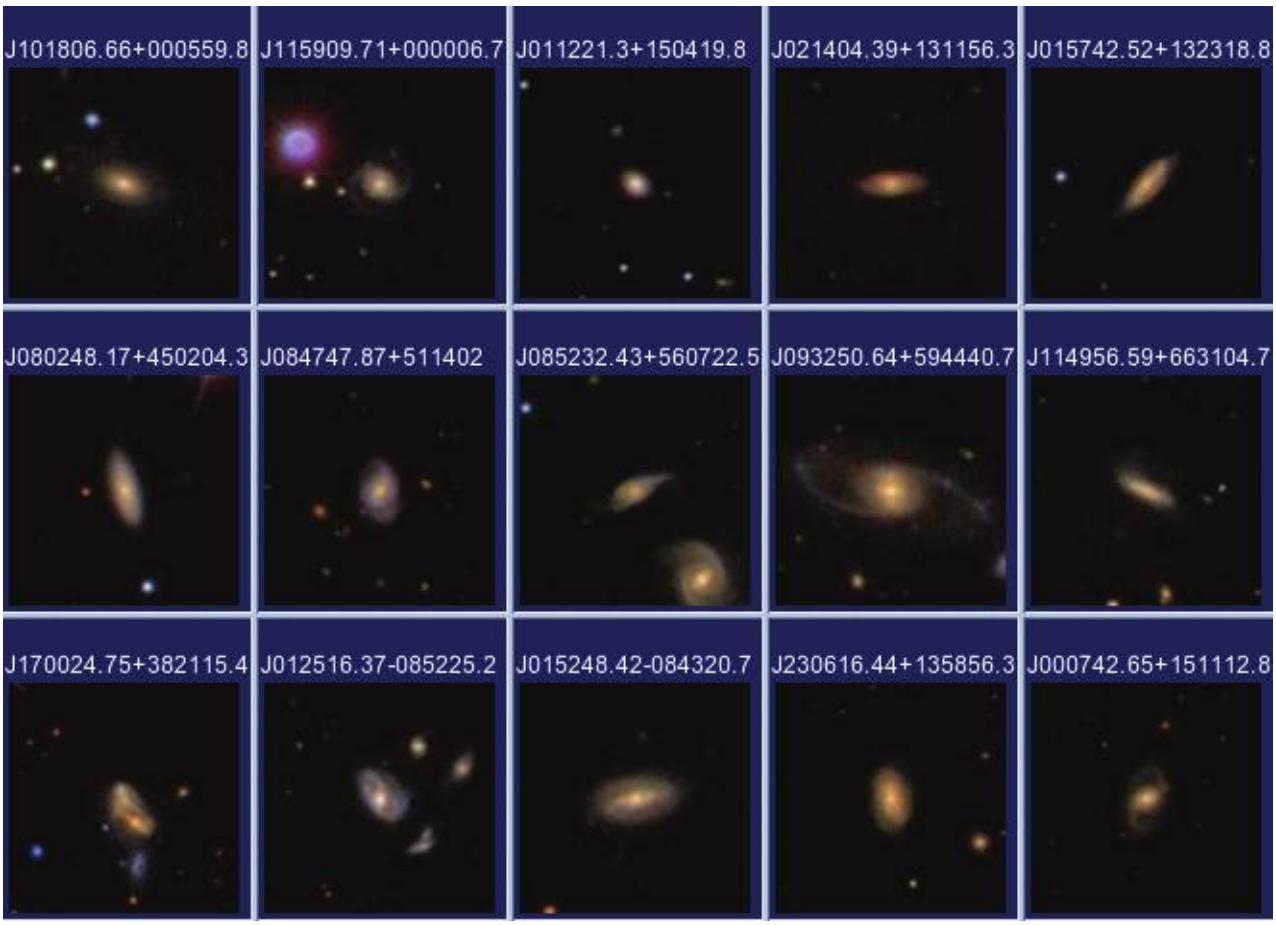

FIG. 8.—SDSS (*first group*) and *GALEX* (*second group*) images of UV-bright galaxies with high central Hα equivalent widths.

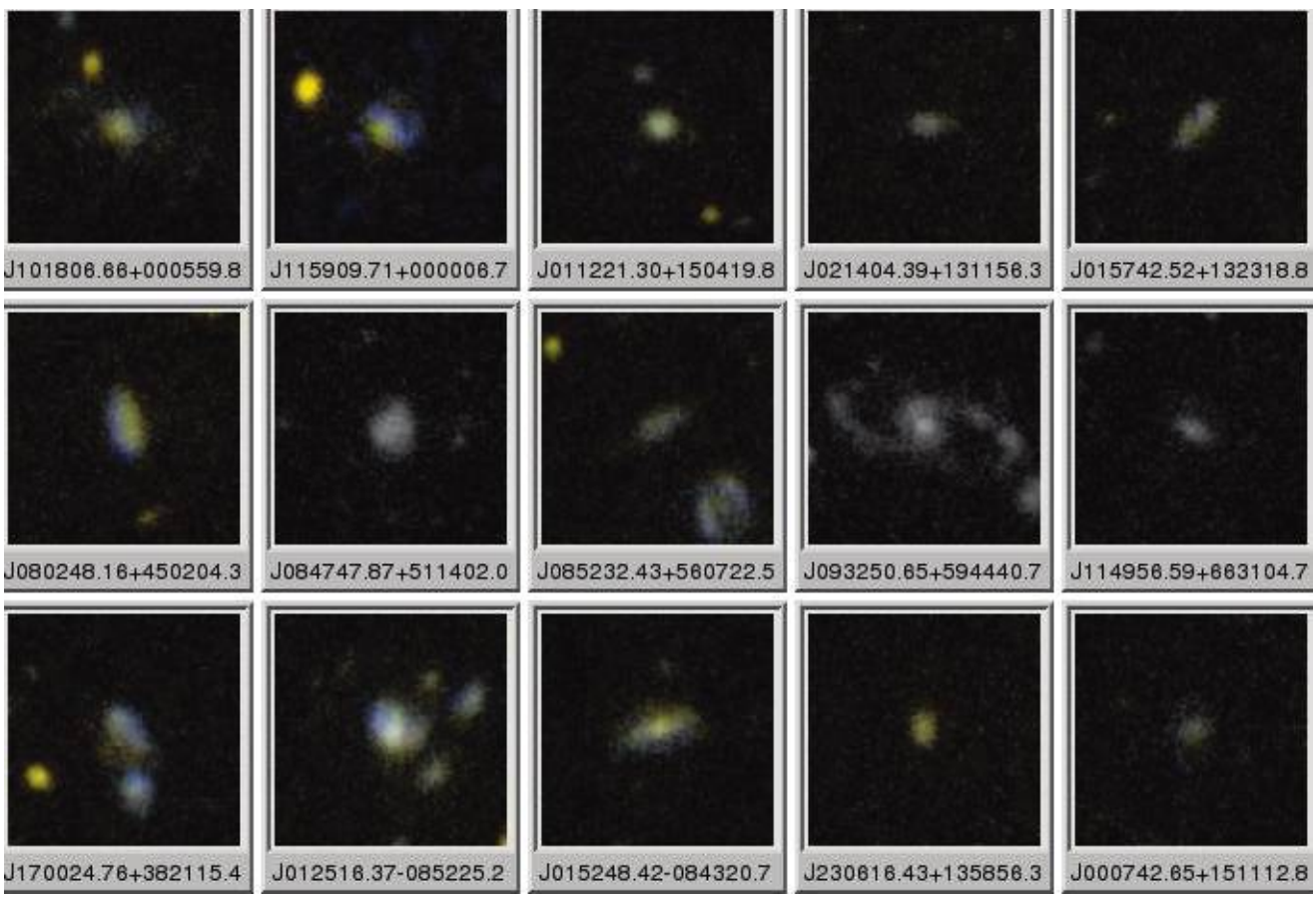

FIG. 8.—*Continued*

FIG. 9.—SDSS (*first group*) and *GALEX* (*second group*) images of UV-faint galaxies.

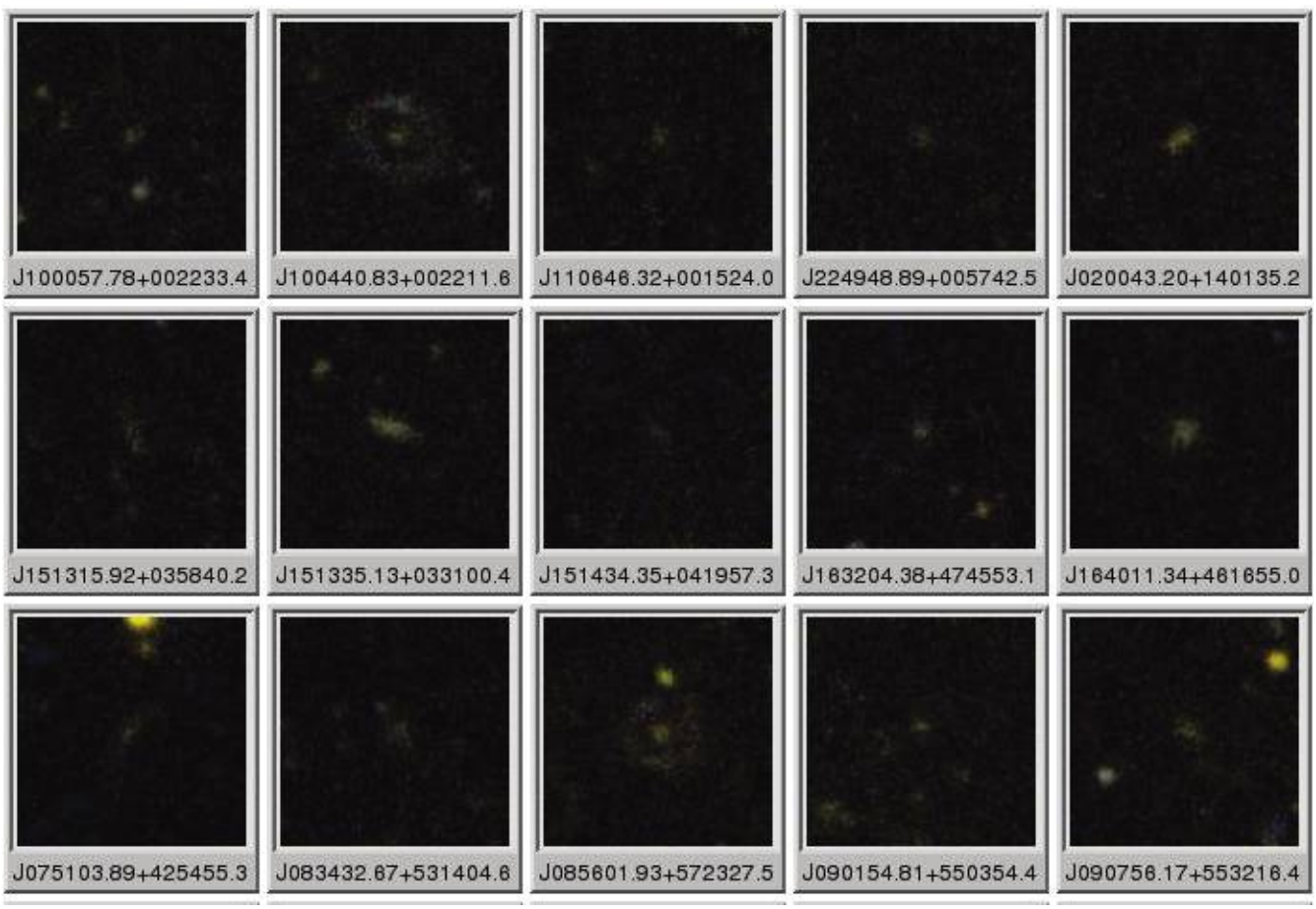

FIG. 9.—*Continued*

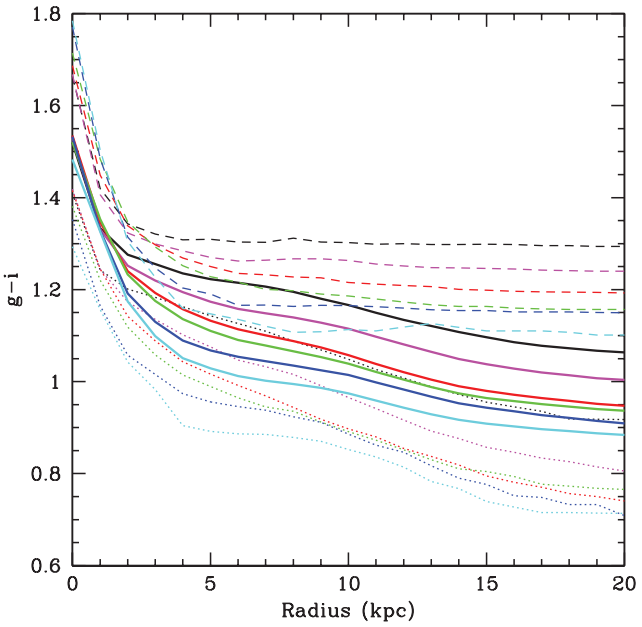

FIG. 10.—Color $g - i$ plotted as a function of physical radius for galaxies in six different ranges of black hole accretion rate, which is parameterized by the quantity log L[O III]/M_{BH}. The black, magenta, red, green, blue, and cyan lines are for AGNs with log L[O III]/M_{BH} in the ranges [< -2.0], [-2, -1.3], [-1.3, -0.6], [-0.6, 0.1], [0.1, 0.7], and [>0.7], respectively. The solid lines show the average profile, while the dashed and dotted lines indicate the 90th and 10th percentiles of the color distribution at a given radius, respectively.

with the continuum luminosity and, by extension, the black hole accretion rate. Assuming that the unified model is valid, the same should hold true in galaxies where the central engine is obscured. In follow-up work, Heckman et al. (2005) studied a sample of hard X-ray–selected AGNs and showed that the hard X-ray emission, which is believed to be an unbiased tracer of accretion on to the black hole, and the [O III] emission-line luminosities were well correlated over a range of 4 orders of magnitudes in luminosity in both type I and type II AGNs. Since we have measurements of the central stellar velocity dispersions for all the galaxies in our sample, we are able to estimate black hole masses using the relations given in Tremaine et al. (2002). The ratio L[O III]/M_{BH} is then a measure of the accretion rate relative to the Eddington rate.

We note that the black hole masses and accretion rates estimated from the SDSS spectra should be regarded as indicative rather than precise measures of these quantities. The stellar velocity dispersions in Tremaine et al. (2002) were measured within physical apertures that were on average a factor of 4 smaller than those corresponding to the 1.5″ fiber diameter for the galaxies in our sample. As discussed in Heckman et al. (2005), there is at least a factor of a few uncertainty in the conversion from an [O III] emission-line luminosity to an accretion rate. Nevertheless, as we demonstrate, the stellar populations of the galaxies in our sample correlate remarkably tightly with L[O III]/M_{BH}.

Less than 15% of the SDSS sample is covered by *GALEX* observations. However, we have seen that even if we lack UV data, we can still use the SDSS $g - i$ color profiles to see whether there are young stars in the outer regions of our galaxies. We have thus chosen to stack galaxies with similar central velocity dispersions in bins of L[O III]/M_{BH} and to study how their optical color profiles change as a function of black hole accretion rate. This is shown in Figure 10 for galaxies with $2.05 < \log \sigma < 2.25$. Solid cyan, blue, green, red, magenta, and black curves show the average $g - i$ color profiles of galaxies hosting AGNs with decreasing values of L[O III]/M_{BH}.[14] The dashed and dotted curves show the upper 90th and lower 10th percentiles of the distribution of $g - i$ color at a given radius. The striking result indicated in this figure is that AGNs with higher accretion rates have bluer colors in their outer regions. In contrast, the average color in the central regions of the galaxy appears to exhibit no dependence on the accretion rate onto the central black hole.

At first sight, this might appear to be a paradoxical result. It would be difficult to come up with any physically motivated scenario that would predict the accretion onto the central black hole to be more strongly modulated by conditions in the outer rather than the inner regions of the galaxy! It is important to remember, however, that galaxy colors are sensitive not only to the ages and metallicities of their stellar populations, but also to the amount of dust present in the interstellar medium. Within the aperture covered by the SDSS fiber aperture, information available from the SDSS spectra allow us to probe mean stellar age and the amount of dust in an independent way. This is illustrated in Figure 11. In the top two panels we plot the distribution of the two age-sensitive indices $D_n(4000)$ and $H\delta_A$ for galaxies in the same ranges in L[O III]/M_{BH} as shown in Figure 10. Here we see a very clear progression in the mean value of these indices as a function of black hole accretion rate. The stellar populations in the central regions of galaxies with strongly accreting black holes are clearly younger. In the bottom panels we plot the distribution of A_z, the attenuation of starlight due to dust in the z band (see Kauffmann et al. 2003a for more details), and the Balmer decrement $H\alpha/H\beta$, which measures the extinction in regions of the galaxy with young, massive stars. Both indicators show that there is more dust in the central regions of galaxies with strongly accreting black holes. We conclude that the reason why the average colors in the central regions of AGN are so weakly correlated with accretion rate is that the bluing that would be expected as a consequence of the decrease in the mean stellar age of the stars in the bulge is canceled by the reddening due to the increase in the amount of dust. The exactness of this cancellation in the central bulge-dominated region of the galaxy is remarkable and is worthy of further consideration. In the outer (presumably disk-dominated) regions of the galaxy, age and dust effects no longer compensate each other exactly and, as a result, these regions of the galaxy do become bluer as the age of the stellar population decreases.

The results presented in Figures 10 and 11 indicate that accretion rates onto central supermassive black holes respond to conditions in *both* the outer and the inner regions of the host galaxies. We now ask whether we can ascertain which response is the stronger of the two. To answer this question, we divide our sample into bins in outer $g - i$ color (measured at radii between 7 and 10 kpc) and in inner stellar population age as measured by the $H\delta_A$ index. We study how the distribution in L[O III]/M_{BH} changes as a function of these measures of the age of the outer and the inner stellar populations. The results are shown in Figures 12 and 13. It is clear from these plots that the accretion rates respond much more strongly to the age of the inner stellar population.

This conclusion is reiterated in Figure 14, where we present the correlations between NUV $- r$ color, $D_n(4000)$, and L[O III]/M_{BH} for galaxies with $2.05 < \log \sigma < 2.25$. As we have discussed, the NUV $- r$ color is sensitive to the age of the stellar population in the outer galaxy (effects due to dust are expected to be weak), $D_n(4000)$ measures the age of the stars in the inner bulge-dominated

[14] Note that we use extinction-corrected values of L[O III] throughout this paper.

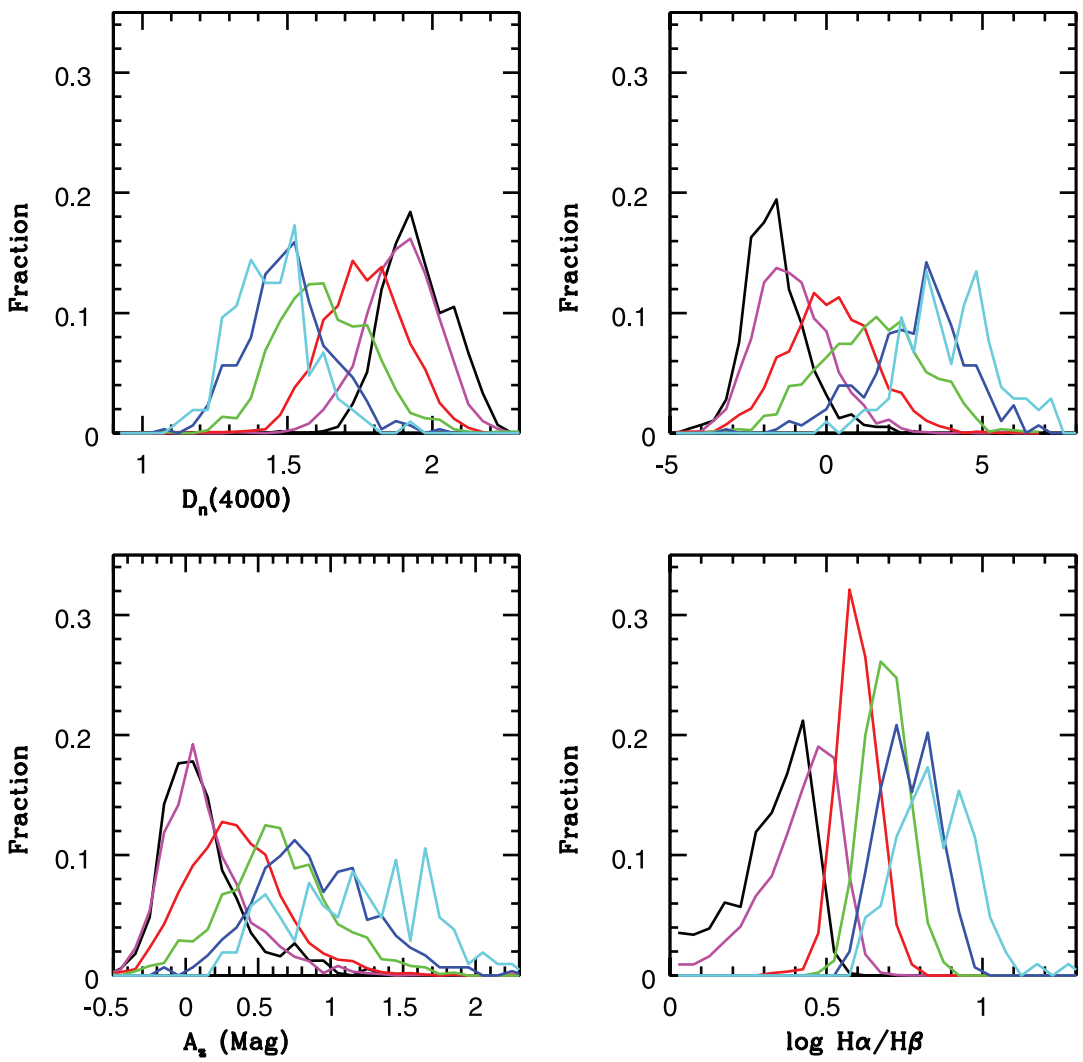

FIG. 11.—Distributions of the age-sensitive spectral indices $D_n(400\ 0)$ and $H\delta_A$, as well as two dust-sensitive measures, in bins of black hole accretion rate parameterized by the quantity $\log L[\mathrm{O\ III}]/M_{\mathrm{BH}}$. The color coding on the curves is the same as in the previous figure.

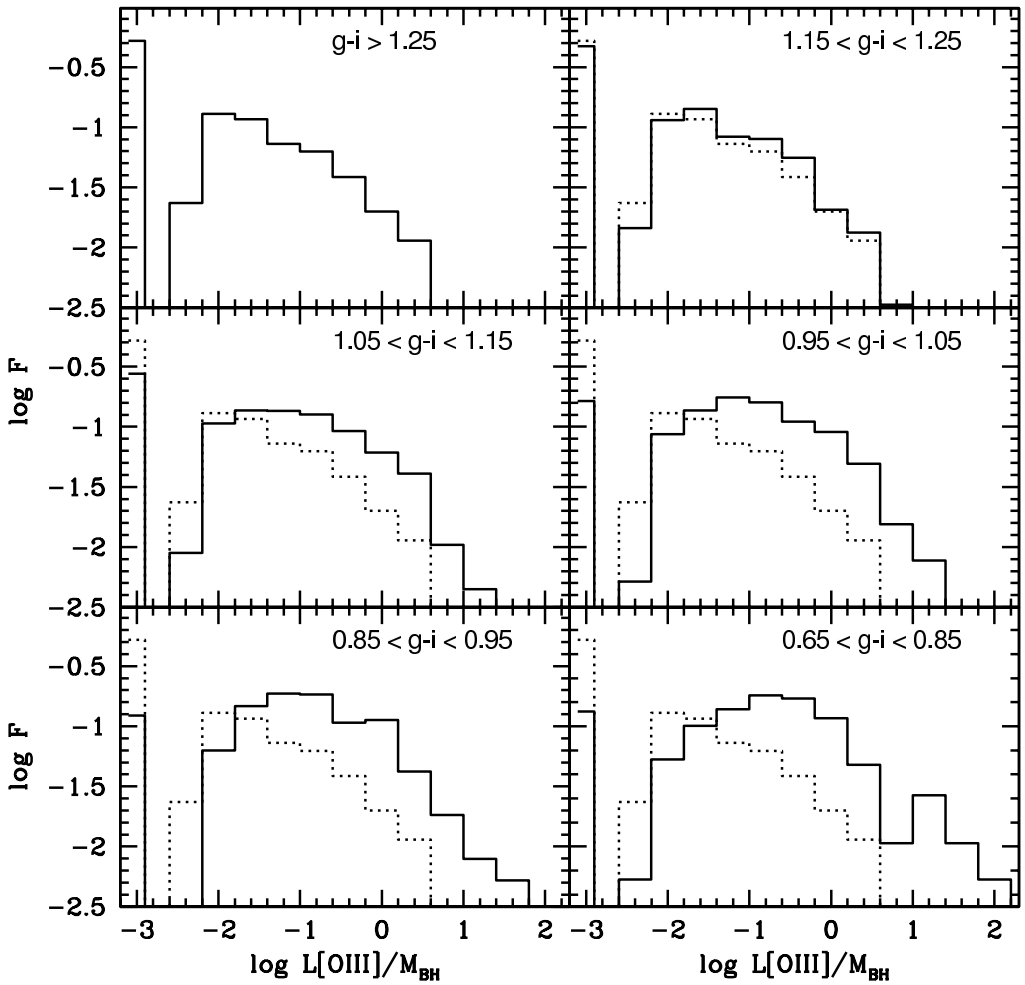

FIG. 12.—Distribution of $\log L[\mathrm{O\ III}]/M_{\mathrm{BH}}$ in bins of outer $g - i$ color. To guide the eye, the distribution shown in the first panel is repeated as a dotted line in each subsequent panel.

region, and $L[\mathrm{O\ III}]/M_{\mathrm{BH}}$ measures the accretion rate onto the black hole. As can be seen, the black hole accretion rate is much more tightly correlated with the mean stellar age in the bulge than in the outer galaxy. The black hole/outer galaxy and bulge/outer galaxy correlations both have a triangular shape. This triangular correlation tells us that galaxies with high black hole accretion rates and young bulges almost always have young stars in their outer regions. However, a young outer region *does not guarantee* that the bulge is young or the black hole accretion rate is high.

6. STELLAR MASS PROFILES

The most straightforward interpretation of the results presented in the previous sections is that the UV light traces an extended reservoir of H I gas that surrounds a subset of the bulge-dominated galaxies in our sample. This outer gas is presumably in the form of a rotationally supported disk, and it contains the fuel that is required for further growth of the the central supermassive black hole and the surrounding bulge. The triangular shape of the correlations between $D_n(4000)$, $L[\mathrm{O\ III}]/M_{\mathrm{BH}}$, and NUV $-$ r color presented in the top two panels of Figure 11 implies that the presence of gas in this disk is a *necessary, but not sufficient, condition for further bulge and black hole growth*. Black holes with low accretion rates are found both in galaxies with old bulges and red NUV $-$ r colors (these are galaxies that are nearly devoid of gas) and in galaxies with old bulges and blue NUV $-$ r colors (these galaxies do contain gas, but in the form of an extended disk). On the other hand, the tight correlation between $L[\mathrm{O\ III}]/M_{\mathrm{BH}}$ and $D_n(4000)$ presented in Figure 14 (*left*) implies that the presence of young stars (and presumably gas) in the bulge is a *necessary and sufficient condition* for further black hole growth. The strong correlation between black hole accretion rate and the amount of extinction measured within the SDSS fiber aperture (Fig. 11, *bottom panels*) is also clear evidence that black hole fuelling is strongly linked to the amount of cold gas in the inner region of the galaxy. We propose that strongly accreting black holes are only found in galaxies where the gas in the disk has become more centrally concentrated, perhaps as a result of angular momentum loss during an interaction.

Unfortunately, H I data are not available for the galaxies in our sample. However, we can test the hypothesis that the extended UV-bright components shown in Figures 7 and 8 correspond to an outer disk by analyzing the radial distribution of the stars in these galaxies. To do this we need to transform the radial surface brightness profile of the galaxy into a stellar mass profile. Bell & de Jong (2001) used spiral galaxy evolution models to predict that the optical colors of galaxies are expected to be strongly correlated with their stellar mass-to-light ratios. Both stellar age and dust attenuation affect the optical colors, but in such a way

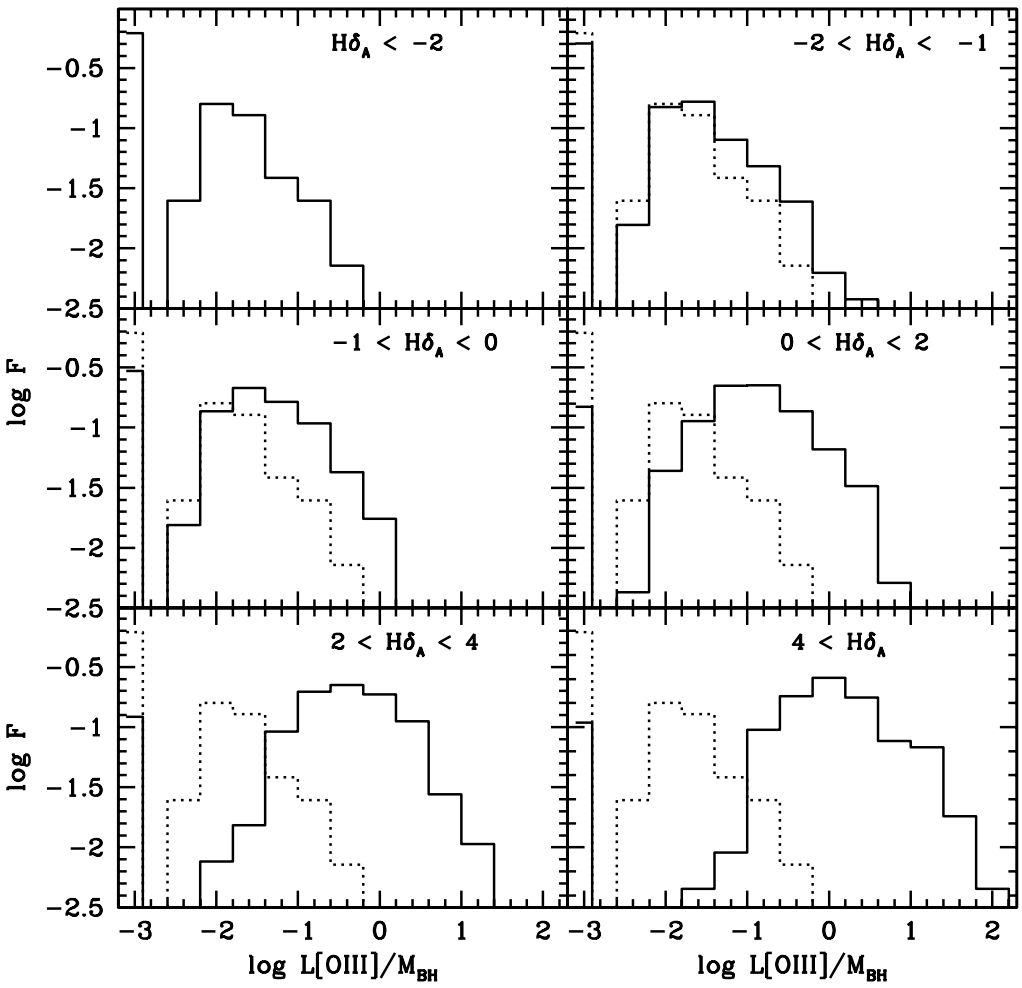

FIG. 13.—Same as Fig. 12, except that the distribution of log L[O III]/$M_{\rm BH}$ is plotted in bins of Hδ_A measured within the fiber.

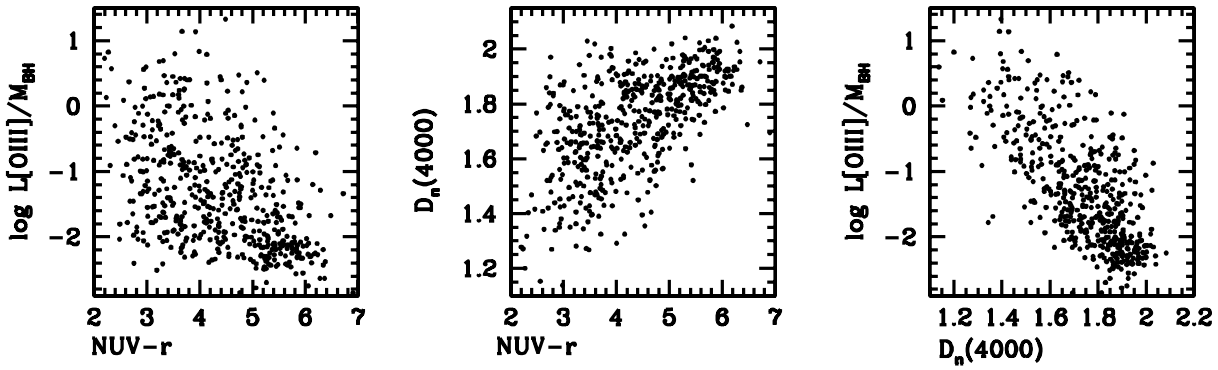

FIG. 14.—Correlations between NUV − r (an indicator of the age of stars in the outer galaxy), $D_n(4000)$ (an indicator of stellar age in the inner galaxy), and L[O III]/M_{BH} (an indicator of accretion rate onto the black hole). *Left*: Black hole vs. disk. *Middle*: Bulge vs. disk. *Right*: Black hole vs. bulge.

that the mass-to-light ratio can still be accurately predicted, provided that the recent star formation history of the galaxy has been reasonably smooth. We have estimated stellar mass-to-light ratios within the SDSS fiber aperture using a method based on stellar absorption-line indices (Kauffmann et al. 2003a). We have correlated our estimates of mass-to-light ratio with a variety of optical colors, and we find the tightest relation with the $g - i$ optical color. This is shown in Figure 15. The black dots show our SDSS/*GALEX* sample of bulge-dominated galaxies, while the blue dots represent galaxies with smaller stellar masses and velocity dispersions but in the same redshift range as the galaxies in our bulge-dominated sample ($0.03 < z < 0.07$). Note that we have taken care to plot the mass-to-light ratio in the i band as a function of the $g - i$ fiber color, so that all quantities are measured and evaluated within the same physical aperture. As can be seen, mass-to-light ratio is well correlated with $g - i$ fiber color over a range of more than a factor 10 in mass-to-light ratio and with an rms scatter of less than 0.1 dex.

This gives us confidence that we can use the i-band surface brightness profile of a galaxy in conjunction with its $g - i$ radial color profile to calculate the fraction of its stellar mass exterior to a given radius in a galaxy. The results of this calculation are shown in Figure 16. We stack galaxies within a narrow range in central stellar velocity disperion ($2.05 < \log \sigma < 2.25$) and study whether their stellar mass profiles differ according to whether they are UV bright or UV faint. In the left panel, solid black and red curves show average mass profiles for UV-faint galaxies, while solid blue and green curves are for UV-bright galaxies. The green curve shows the mass profile for UV-bright galaxies with weak central emission-line strengths, while the blue curve is for UV-bright galaxies with strong central emission lines. (Note that the color coding is the same as in Fig. 6.) As can be seen, the stellar mass profiles of the UV-faint galaxies and the UV-bright galaxies with strong central emission-line strengths are very similar. Only UV-bright galaxies with weak central emission lines have significantly different mass profiles; these galaxies have on average 10% more mass in their outer regions.

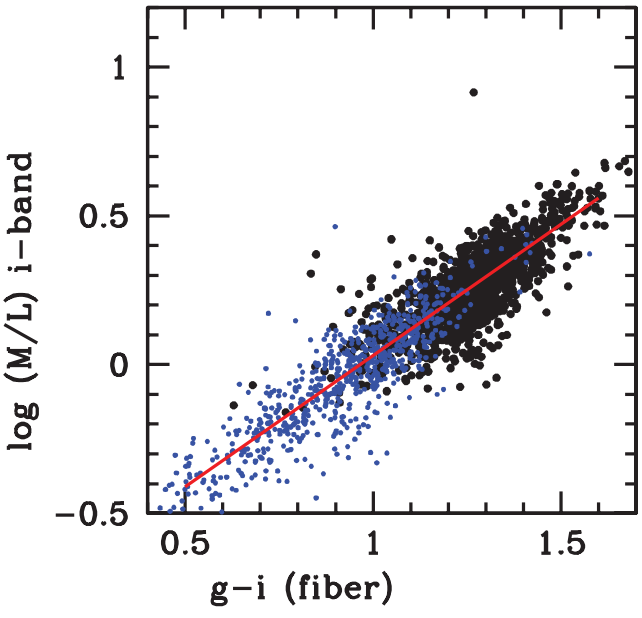

FIG. 15.—The i-band mass-to-light ratio estimated using stellar absorption line indices, plotted as a function of $g - i$ fiber color.

In Figure 16 (*right panel*), we plot the stellar mass profiles of AGNs ordered according black hole accretion rate. The color coding is the same as in Figure 10. There is a trend for galaxies with higher black hole accretion rates to have more concentrated stellar mass profiles, but it is quite weak. Only the galaxies with black holes that are accreting near the Eddington rate appear significantly more concentrated. Note that these strongly accreting systems also have total stellar masses that are about 10%–20% smaller than the galaxies with weakly accreting black holes. The small difference in total stellar mass at fixed value of the central velocity dispersion σ is consistent with the notion that these galaxies all have very similar total masses but that the more strongly accreting objects have slightly higher gas fractions.

The evolutionary scenario suggested by the results presented in this section is one in which bulges and their central supermassive black holes form from gas located in an outer disk. These disks have presumably accreted from gas in the surrounding dark matter halo. So long as the galaxy remains undisturbed, very little of the gas from this disk will manage to reach the bulge and fuel an AGN. These quiescent bulges/black holes with blue extended disks make up the left bottom corner of the triangular cloud of dots shown in the left and middle panels of Figure 14. Eventually, some process will lead to a flow of gas from the disk to the bulge. This triggers star formation in the bulge and significant growth of the central black hole. During this process, the increase of stellar mass in the bulge is larger than the increase in the disk, so the galaxy develops a more centrally concentrated stellar mass profile. Once the gas in the disk is exhausted, the mass profile of

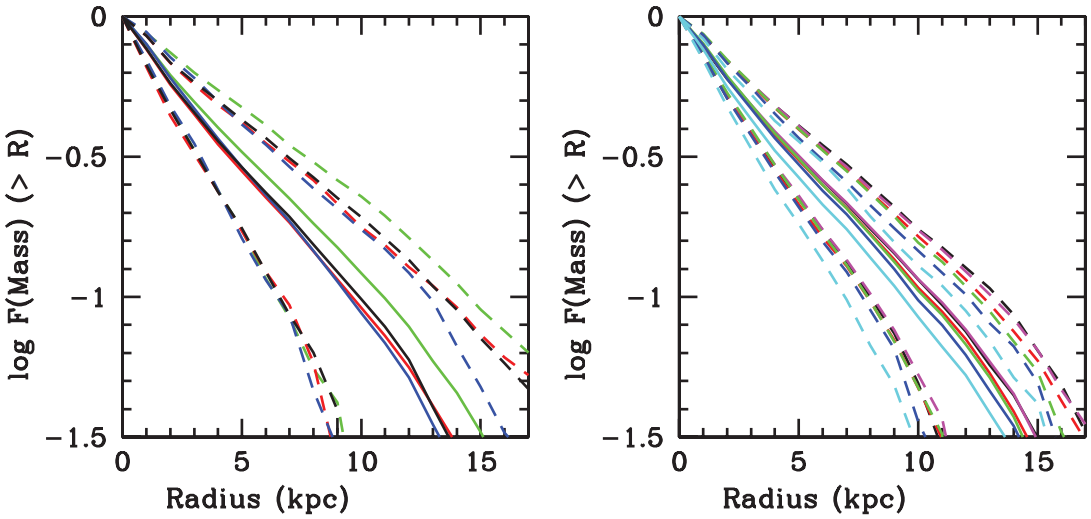

FIG. 16.—*Left*: Fraction of stellar mass exterior to a given radius is plotted as a function of radius. The definition of the colored lines is the same as in Fig. 9. The solid lines show the average stellar mass profiles. The dashed lines indicate the lower 10th and upper 90th percentiles of the external mass at a given value of R. UV-bright galaxies with little star formation in their bulges have the most extended stellar mass profiles. *Right*: Same as the left panel, except that the definition of the colored lines is the same as in Fig. 10. Galaxies with the highest values of L[O III]/$M_{\rm BH}$ have the most concentrated stellar mass profiles.

the galaxy is indistinguishable from that of a classical elliptical galaxy.

7. SUMMARY AND CONCLUSIONS

We have defined a sample of massive bulge-dominated galaxies with both *GALEX* photometry and spectroscopic data from the SDSS. Our choice of limiting r-band magnitude ensures that that the sample is complete in the near ultraviolet passband. We have also imposed stellar mass and redshift cuts to ensure that the sample is volume-limited for all galaxies above $10^{10.4}\ M_{\odot}$ irrespective of their past star formation histories and present-day stellar mass-to-light ratios. We study galaxies with central velocity dispersions greater than 100 km s^{-1}. We have shown that these are bulge-dominated systems with stellar surface mass densities well above the value where galaxies transition from actively star-forming to "passive" systems. The NUV data provide significantly higher sensitivity to low rates of star formation in bulge-dominated galaxies. Our primary observational results can be summarized as follows:

1. Bulge-dominated galaxies exhibit a much larger spread in NUV $-$ r color than in optical $g - r$ color. The dispersion in color decreases for galaxies with larger central velocity dispersions.
2. Nearly all of the galaxies with blue NUV $-$ r colors are AGNs.
3. *GALEX* images and SDSS color profiles demonstrate that the UV excess is associated primarily with an extended outer component of the galaxy.
4. When comparing fiber-based properties to global ones, we find "triangular" correlations. Galaxies with red outer regions almost never have a strong AGN or a young bulge. Galaxies with blue outer regions have a wide range in bulge/black hole properties. Galaxies with strongly accreting black holes and young bulges almost always have blue outer regions.
5. The black hole growth rate correlates much more strongly with the age of the stellar population in the bulge than in the outer region of the galaxy.
6. The amount of extinction in the bulge (tracing the column density of the cold interstellar medium) is also strongly linked to black hole growth and the age of the bulge stars.
7. At fixed central stellar velocity dispersion, we find that the radial distribution of the stellar mass in the host galaxy shows only small ($\sim$10%) variations as a function of black hole growth rate and the color of the disk.

The suggested scenario is one in which the source of gas that builds the bulge and black hole is a relatively low-mass reservoir of cold gas in the disk. The presence of the gas is necessary but not sufficient for bulge and black hole growth. Some mechanism must transport this gas inward in a time-variable way. The duty cycle for such inflow periods (once cold gas in the outer disk is present) must be relatively large, because a significant fraction of the galaxies in our sample have both blue outer disks and star formation in the bulge. After the gas has been transported into the bulge, the relative timescales for bulge and black hole growth must be also similar, because there is a reasonably tight correlation between $D_n(4000)$ and L[O III]/$M_{\rm BH}$.

The disk gas itself is likely to be the result of the accretion of gas from an external source. It is possible that these disks represent the repository of baryonic material that has managed to condense out of cooling flows in the centers of dark matter halos. As this gas is converted into stars in the bulge and disk, galaxies will turn red in NUV $-$ r. Further inflow can bring them back into the blue NUV $-$ r sequence. One question that arises is whether the evolution of the disk occurs through secular processes, i.e., the required rearrangement of angular momentum and mass is achieved through collective phenomena such as bars, oval disks, spiral structure, and triaxial dark matter halos (see Kormendy & Kennicutt 2004 for a recent review), or whether the evolution is dominated by more violent and rapid processes, such as mergers and strong interactions. The similarity of the average stellar mass profiles of the quiescent and active galaxies implies that the processes that lead to episodic growth of the bulge and black hole do not usually involve major changes in the galaxy structure. We will address these issues in future work.

In summary, the *GALEX* data presented in this paper have provided us with a new view of the bulge-dominated galaxy population in which star formation has largely shut down by the present day. We have learned that the transition from actively star-forming galaxies at low stellar surface mass densities to "passive" galaxies

at high stellar surface densities does not imply that disk formation has ceased altogether, but that disks have become subdominant. In galaxies with large central velocity dispersions, the disks are inconspicuous in the optical. However, star-forming outer disks still dominate the energy output of the galaxy at ultraviolet wavelengths, and this leads to a very different accounting of which galaxies in the local universe are truly "red and dead." We have also seen that these UV disks contain the fuel for continued growth of central supermassive black holes. Understanding the processes by which UV-bright disks form and why their formation is increasingly inhibited as the central velocity dispersion of the bulge increases will be an important next step in piecing together the puzzle of how massive galaxies came to be.

GALEX (*Galaxy Evolution Explorer*) is a NASA Small Explorer, launched in 2003 April. We gratefully acknowledge NASA's support for construction, operation, and science analysis for the *GALEX* mission, developed in cooperation with the Centre National d'Etudes Spatiales (CNES) of France and the Korean Ministry of Science and Technology. Funding for the creation and distribution of the SDSS Archive has been provided by the Alfred P. Sloan Foundation, the Participating Institutions, the National Aeronautics and Space Administration, the National Science Foundation, the US Department of Energy, the Japanese Monbukagakusho, and the Max Planck Society. The SDSS Web site is http://www.sdss.org. The SDSS is managed by the Astrophysical Research Consortium for the Participating Institutions. The Participating Institutions are the University of Chicago, Fermilab, the Institute for Advanced Study, the Japan Participation Group, the Johns Hopkins University, the Korean Scientist Group, Los Alamos National Laboratory, the Max Planck Institute for Astronomy, the Max Planck Institute for Astrophysics, New Mexico State University, the University of Pittsburgh, the University of Portsmouth, Princeton University, the US Naval Observatory, and the University of Washington.

REFERENCES

Adelman-McCarthy, J. K., et al. 2006, ApJS, 162, 38
Bell, E. F., & de Jong, R. S. 2001, ApJ, 550, 212
Bernardi, M., et al. 2003, AJ, 125, 1849
Best, P. N., Kauffmann, G., Heckman, T. M., Brinchmann, J., Charlot, S., Ivezić, Ž., & White, S. D. M. 2005, MNRAS, 362, 25
Boselli, A., et al. 2005, ApJ, 629, L29
Bower, R. G., Lucey, J. R., & Ellis, R. S. 1992, MNRAS, 254, 601
Brinchmann, J., Charlot, S., White, S. D. M., Tremonti, C., Kauffmann, G., Heckman, T., & Brinkmann, J. 2004, MNRAS, 351, 1151
Bruzual, G., & Charlot, S. 2003, MNRAS, 344, 1000
Cardelli, J. A., Clayton, G. C., & Mathis, J. S. 1989, ApJ, 345, 245
Cardiel, N., Gorgas, J., & Aragon-Salamanca, A. 1998, MNRAS, 298, 977
Churazov, E., Brüggen, M., Kaiser, C. R., Böhringer, H., & Forman, W. 2001, ApJ, 554, 261
Crawford, C. S., Allen, S. W., Ebeling, H., Edge, A. C., & Fabian, A. C. 1999, MNRAS, 306, 857
Croton, D. J., et al. 2006, MNRAS, 365, 11
Di Matteo, T., Springel, V., & Hernquist, L. 2005, Nature, 433, 604
Granato, G. L., De Zotti, G., Silva, L., Bressan, A., & Danese, L. 2004, ApJ, 600, 580
Heckman, T. M., Kauffmann, G., Brinchmann, J., Charlot, S., Tremonti, C., & White, S. D. M. 2004, ApJ, 613, 109
Heckman, T. M., Ptak, A., Hornschemeier, A., & Kauffmann, G. 2005, ApJ, 634, 161
Hicks, A. K., & Mushotzky, R. 2005, ApJ, 635, L9
Kauffmann, G., Heckman, T. M., De Lucia, G., Brinchmann, J., Charlot, S., Tremonti, C., White, S. D. M., & Brinkmann, J. 2006, MNRAS, 367, 1394
Kauffmann, G., White, S. D. M., & Guiderdoni, B. 1993, MNRAS, 264, 201
Kauffmann, G., et al. 2003a, MNRAS, 341, 33
Kauffmann, G., et al. 2003b, MNRAS, 341, 54
———. 2003c, MNRAS, 346, 1055
Kaviraj, S., Devriendt, J. E. G., Ferreras, I., & Yi, S. K. 2005, MNRAS, 360, 60
Kaviraj, S., et al. 2006, ApJS, 173, 619
Kormendy, J., & Kennicutt, R. C., Jr. 2004, ARA&A, 42, 603
Lupton, R., Blanton, M. R., Fekete, G., Hogg, D. W., O'Mullane, W., Szalay, A., & Wherry, N. 2004, PASP, 116, 133
Martin, D. C., et al. 2005, ApJ, 619, L1
———. 2006, ApJS, submitted
McNamara, B. R. 2004, in The Riddle of Cooling Flows in Galaxies and Clusters of Galaxies, ed. T. Reiprich, J. Kempner, & N. Soker (Charlottesville: Univ. Virginia), 177
McNamara, B. R., & O'Connell, R. W. 1989, AJ, 98, 2018
Morrissey, P., et al. 2005, ApJ, 619, L7
Popescu, C. C., et al. 2005, ApJ, 619, L75
Renzini, A. 2006, ARA&A, 44, 141
Rich, R. M., et al. 2005, ApJ, 619, L107
Ruszkowski, M., Brüggen, M., & Begelman, M. C. 2004, ApJ, 611, 158
Schawinski, K., et al. 2007, ApJS, 173, 512
———. 2006, Nature, 442, 888
Schlegel, D. J., Finkbeiner, D. P., & Davis, M. 1998, ApJ, 500, 525
Seibert, M., et al. 2005, ApJ, 619, L23
Shimasaku, K., et al. 2001, AJ, 122, 1238
Strateva, I., et al. 2001, AJ, 122, 1861
Thilker, D. A., et al. 2005, ApJ, 619, L79
Tremaine, S., et al. 2002, ApJ, 574, 740
Tremonti, C. A., et al. 2004, ApJ, 613, 898
Yi, S. K., et al. 2005, ApJ, 619, L111